

Sources of geomagnetic storms for solar minimum and maximum conditions during 1972-2000

I. G. Richardson¹

NASA Goddard Space Flight Center, Greenbelt, Maryland

E. W. Cliver

Air Force Research Laboratory, Hanscom Air Force Base, Bedford, Massachusetts

H. V. Cane²

NASA Goddard Space Flight Center, Greenbelt, Maryland

Abstract. We determine the solar wind structures (coronal mass ejection (CME) - related, corotating high-speed streams, and slow solar wind) driving geomagnetic storms of various strength over nearly three solar cycles (1972 - 2000). The most intense storms (defined by Kp) at both solar minimum and solar maximum are almost all ($\sim 97\%$) generated by transient structures associated with CMEs. Weaker storms are preferentially associated with streams at solar minimum and with CMEs at solar maximum, reflecting the change in the structure of the solar wind between these phases of the solar cycle. Slow solar wind generates a small fraction of the weaker storms at solar minimum and maximum. We also determine the size distributions of Kp for each solar wind component.

1. Introduction

Recently [Richardson *et al.*, 2000], we quantified the contribution of different solar wind components (CME-related structures, corotating high-speed streams, and slow solar wind) to long-term averages of the aa geomagnetic index during 1972 - 1986. In this related study, we investigate the association of these solar wind components with individual geomagnetic storms. Although the solar wind drivers of geomagnetic storms have been discussed previously for limited intervals and with an emphasis on intense storms [e.g., Gosling *et al.*, 1991; Tsurutani and Gonzalez, 1997; and references therein], we consider storms of all sizes which occurred over an extended period (1972 - 2000) spanning nearly three solar cycles and compare the drivers at solar maximum and solar minimum. We also compare the distributions of Kp for each solar wind component at solar maximum and minimum.

2. Data Analysis

Our identification of solar wind components is outlined in Richardson *et al.* [2000]. Briefly, we examined near-Earth

¹Also at Department of Astronomy, University of Maryland, College Park.

²Also at School of Mathematics and Physics, University of Tasmania, Hobart, Australia.

Copyright 2001 by the American Geophysical Union.

Paper number 2001GL013052.
0094-8276/01/2001GL013052\$05.00

solar wind data from the National Space Science Data Center OMNI database and classified the solar wind into four categories: “CME-associated” (embracing “ejecta” (the interplanetary material associated with CMEs at the Sun), transient forward shocks generated by fast ejecta, and post-shock flows); corotating solar wind streams from coronal holes [Belcher and Davis, 1971]; slow ($< \sim 400$ km/s), inter-stream solar wind; and “uncertain” (e.g., insufficient data or could not be included in another category). The OMNI data have variable coverage. Thus, our analysis starts in 1972 when observations become reasonably complete. From the mid-1980s until late 1994, there are regular, several-day gaps in the OMNI data which hamper our ability to classify solar wind structures. To supplement the OMNI data, other data have been considered. For example, geomagnetic storm sudden commencements help to identify interplanetary shocks. Energetic particle observations indicate shocks and ejecta associated with energetic solar events/CMEs [e.g., Cane *et al.*, 1996] and cosmic ray modulations associated with corotating streams [e.g., Richardson *et al.*, 1999]. For recent periods, solar wind observations from the ACE spacecraft have also been considered. Ejecta are identified from typical ejecta signatures [e.g., Gosling, 1990; Richardson and Cane, 1995] such as “magnetic clouds”, bidirectional solar wind heat flux electrons, bidirectional energetic ~ 1 MeV ions, and intervals of abnormally low plasma proton temperatures. We have also incorporated results from our previous ejecta studies [e.g., Cane *et al.*, 1996, 2000]. By combining these various data sets, we have been able to make a reasonably complete classification of the solar wind structures at Earth.

3. Solar Wind Structures Associated With Geomagnetic Storms

To identify storm conditions, we used the criteria of Gosling *et al.* [1991] based on the 3-hour Kp index (0 = lowest activity; 9 = most intense activity). A “major” storm has maximum Kp ($Kp\text{-max}$) $\geq 8_-$, together with $Kp \geq 6_-$ for at least three 3-hour intervals in a 24-hour period. A “large” storm has $7_- \leq Kp\text{-max} \leq 7_+$ and $Kp \geq 6_-$ for at least three 3-hour intervals in a 24-hour period. “Medium” storms are all others with $Kp\text{-max} \geq 6_-$, while “small” storms have $5_- \leq Kp\text{-max} \leq 5_+$. For each storm, we identified the solar wind component generating the storm. Note

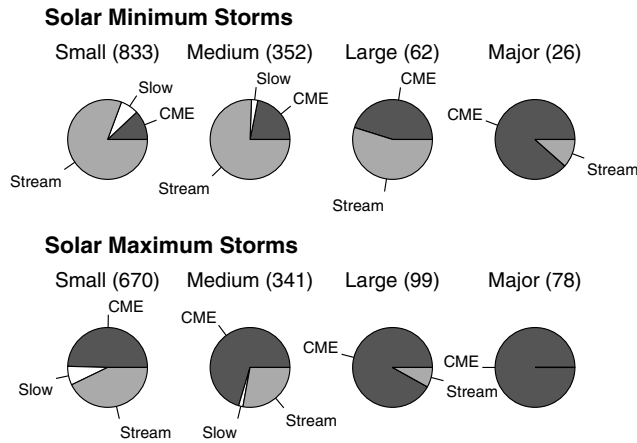


Figure 1. Pie plots summarizing the fraction of small, medium, large and major geomagnetic storms (as defined in the text) associated with CME-related solar wind structures, corotating streams, and slow solar wind, for periods around solar minima (top row) and solar maxima (bottom row) in 1972-2000. Storms for which the solar wind structure is uncertain are excluded from the pie plots. The numbers of storms in each plot is given in parentheses.

that these criteria identify intervals when storm conditions prevail, rather than discrete storms characterized by a rise then fall in activity and some maximum activity level. Thus, an intense storm, generated say by a CME, which extends over several days may contribute to more than one interval of storm conditions. We would assign all these storm intervals as “CME-associated”. We divided the analysis period into intervals around solar minimum (1973 - 1977; 1983 - 1987; 1993 - 1997) and solar maximum (1972; 1978 - 1982; 1988 - 1992; 1998 - 2000) since, as will be shown below, the types of structure associated with storms depend on solar activity levels.

Figure 1 summarizes the solar wind components associated with each category of storm. Since these associations are found to be fairly consistent from cycle to cycle, the results presented here are summed over all solar minimum (top row) and solar maximum intervals (bottom row). The results in Figure 1 are also listed in Table 1. The $\sim 10\%$ of storms for which the solar wind structure is uncertain (Table 1) are excluded from the pie plots. These tend to be weaker storms, since the drivers of strong storms can more often be inferred from other observations in the absence of

in-situ solar wind data. The number of storms in each pie plot is given in parentheses. There is a clear difference in the associations between solar minimum and solar maximum. Around solar minimum, we find that: (a) $\sim 80\%$ of small storms are associated with streams, $\sim 12\%$ with CMEs and $\sim 7\%$ with slow solar wind; (b) \sim three quarters of medium storms are associated with streams, and \sim one-quarter with CMEs; (c) \geq one-half of large storms are associated with streams and \leq one-half with CMEs, and (d) $\sim 90\%$ of major storms are associated with CMEs, the remainder with streams. Examples of major storms associated with streams are May 14, 1973, and April 7, 1995.

Around solar maximum, (a) \sim one-half of small storms are associated with CMEs, $\sim 40\%$ with streams, and $\sim 10\%$ with slow solar wind. There are fewer such storms at solar maximum than at solar minimum; (b) $\sim 70\%$ of medium storms are associated with CMEs, the remainder predominantly with streams; (c) $\sim 90\%$ of large storms are associated with CMEs; (d) All major storms are CME-associated, and such storms are more frequent than at solar minimum. Thus, the major change is the enhanced importance of CMEs relative to streams in generating weaker storms at solar maximum.

Figure 2 shows the yearly occurrence rate of small, medium, and large + major storms during 1972-2000 associated with CMEs (\bullet) and streams (\circ). The sunspot number is shown in the top panel. Small, medium and, to a lesser extent, large/major storms are associated with streams as well as with CMEs. Storms associated with CMEs are predominant around solar maximum. Those associated with streams are most prevalent during the decay phase of the solar cycle but are not completely absent around solar maximum. Figures 1 and 2 provide further confirmation of the division of geomagnetic storms into two classes that was established by the mid-1940s, i.e., “sporadic”, now known to be associated with CMEs, and “recurrent”, associated with corotating streams (see *Cliver* [1995] for a historical review).

4. Size Distributions of Kp in Solar Wind Components

We now determine the size distributions of Kp associated with the CME-related, corotating stream and slow solar wind components around solar maximum and solar minimum. Figure 3 shows the occurrence frequency of Kp (number of 3-hr intervals with a given Kp divided by the number of intervals for all Kp in the given solar wind com-

Table 1. Association of Geomagnetic Storms and Solar Wind Components in 1972-2000

	Storm Size	Events	CME-Associated	Corotating Stream	Slow S. W.	Uncertain Events
Solar Minimum:	Small	833 ^a	12% ^a	81%	7%	83
	Medium	352	22%	76%	3%	30
	Large	62	45%	54%	0%	1
	Major	26	88%	12%	0%	4
Solar Maximum:	Small	670	50%	43%	8%	93
	Medium	341	70%	28%	2%	33
	Large	99	92%	8%	0%	3
	Major	78	100%	0%	0%	1

^aExcluding “Uncertain” events.

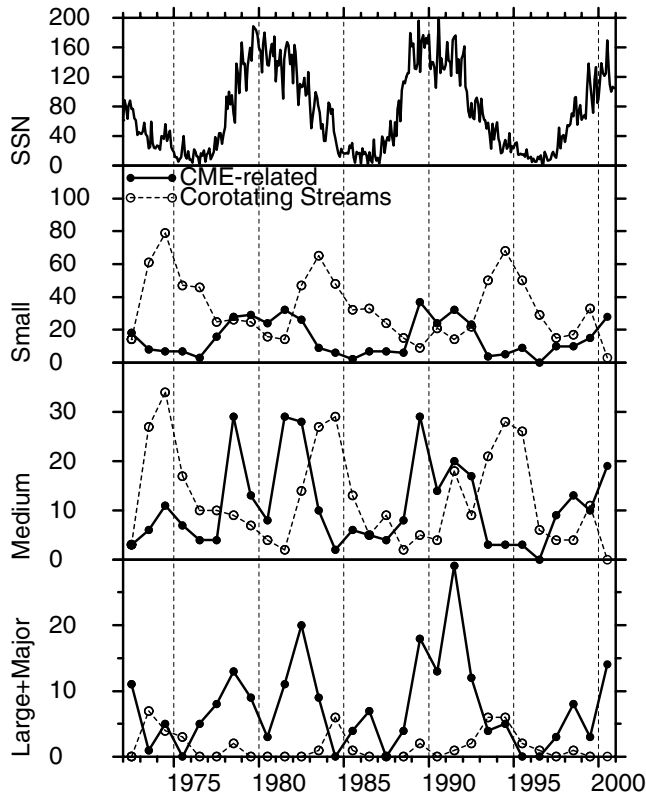


Figure 2. Occurrence rates (storms/year) of small, medium and large + major storms in 1972-2000 associated with CMEs and corotating streams. The sunspot number is shown in the top panel.

ponent). Distributions for solar minimum (\bullet) and maximum (\circ) are shown in each panel. The distributions are broad and encompass a wide range of Kp values. They evidently vary with the type of solar wind structure, but are largely uninfluenced by solar activity levels. The most probable Kp in CME-associated structures is $Kp \sim 3$, compared with $Kp \sim 2-3$ in streams and $Kp \sim 1$ in slow solar wind. There is a larger tail of high Kp values associated with CMEs. Even for slow solar wind though, the tail of the distribution extends to $Kp \sim 5$. These higher activity levels are typically associated with significant southward magnetic fields, such fields being conducive to the generation of geomagnetic activity.

An interesting way to compare these distributions further is to plot the percentage of all the occurrences of a particular Kp value associated with each solar wind component (Figure 4). Results for solar minimum and solar maximum are shown in the top and middle panels respectively. The curves in each panel correspond to CME-related (\bullet), streams (\circ) and slow solar wind (*). Thus, at both activity levels, the majority of high Kp values are associated with CMEs. However, we emphasize that (as Figure 3 demonstrates), this does not mean that CMEs are typically associated with high levels of geomagnetic activity. Streams make a major contribution to intermediate values of Kp (~ 4), whereas slow solar wind accounts for the majority of low Kp . There are two conspicuous differences between solar minimum and maximum: the larger fraction of mid-range values of Kp ($\sim 2-6$) associated with streams at solar minimum, and the

generally higher fraction of all Kp values associated with CMEs at solar maximum.

The bottom panel of Figure 4 shows the Kp distributions expressed in a further way. Here, the probability of equaling or exceeding a given Kp in each type of solar wind is shown. (The results summarize the complete analysis period since they vary only slightly with solar cycle phase (cf. Figure 3)). Again, although the probability of reaching high Kp values is greatest for CME-associated structures, it is evident that only a small subset of such structures are accompanied by strong geomagnetic activity.

5. Summary and Discussion

We have identified the solar wind structures at Earth which generated geomagnetic storms during nearly three solar cycles. The strongest storms are predominantly, but not exclusively related to CMEs. Streams can occasionally generate strong storms around solar minimum. The majority of intermediate strength storms are related to streams at solar minimum and to CMEs at solar maximum. Weak storms are predominantly associated with streams at solar minimum, and are most prominent during the decay of the solar cycle. At solar maximum, they are generated by both streams and CMEs. These changes reflect differences in the fraction of the solar wind at Earth occupied by the various solar wind components around solar minimum and maximum [Richardson *et al.*, 2000].

Our results are consistent with Gosling *et al.* [1991], who found that essentially all large and major storms at solar maximum are associated with CMEs and the shocks that they generate. (Note that Gosling *et al.* [1991] sub-divided such storms into three categories depending on whether they were generated by the ejecta or the post-shock flow

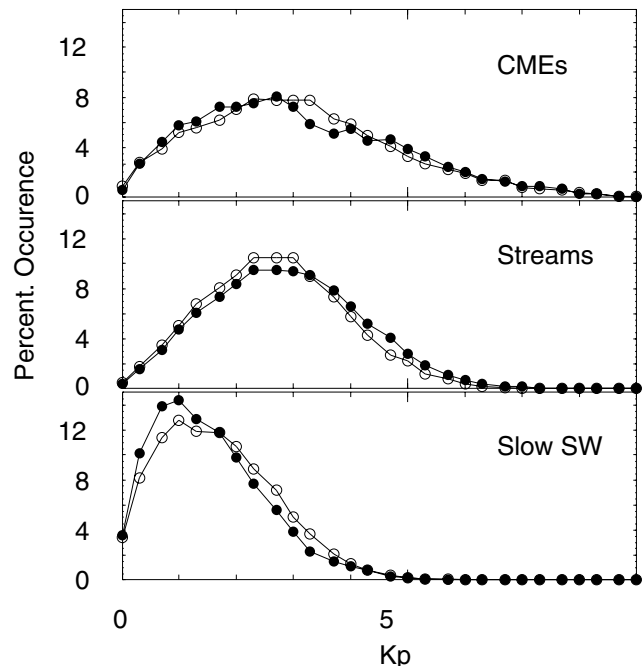


Figure 3. Occurrence (%) of Kp values for CME-associated structures (top panel), corotating streams (second panel), and slow solar wind (bottom panel), around solar minimum (\bullet) and solar maximum (\circ).

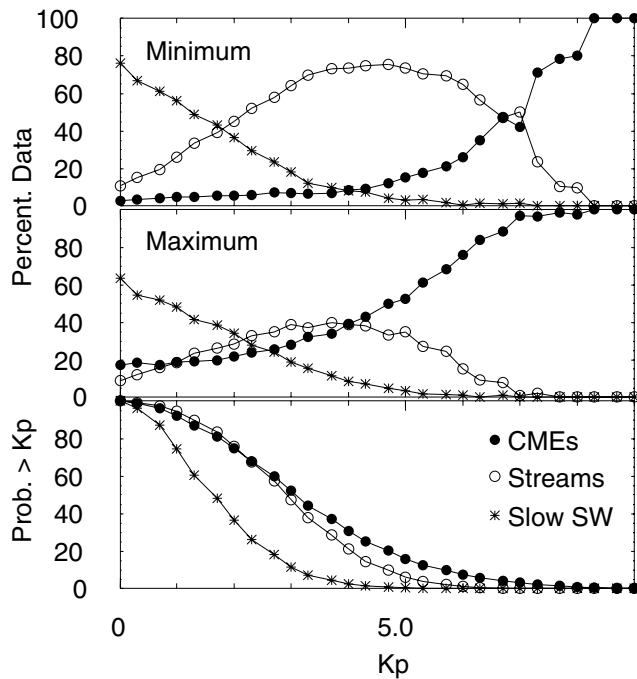


Figure 4. Fraction (%) of all occurrences of a given Kp associated with each type of solar wind, for solar minimum (top) and solar maximum (middle) periods in 1972-2000. Bottom panel: Probability (%) of Kp equaling or exceeding a given value in each type of solar wind, for the complete analysis interval.

or by a combination of these flows.) However, they found smaller fractions of small and medium storms associated with CMEs ($\sim 20\%$ and $\sim 50\%$ respectively) than we obtain ($\sim 50\%$ and $\sim 70\%$). A possible reason for this difference is that we have considered a wider range of ejecta signatures. Small/medium storms during the decay of intense CME-associated storms will also enhance the number of such events associated with CMEs.

Although CMEs evidently do generate the most important storms, it nonetheless should be emphasized that CME-associated structures generate a wide range of activity levels and do not necessarily give rise to major storms (see also Gosling *et al.* [1991]). Thus, a high false alarm rate will inevitably result if it is presumed that an Earthward-directed CME, detected for example by coronagraphs, will result in significant geomagnetic activity [St. Cyr *et al.*, 2000]. Additional information, in particular the configuration of the embedded magnetic fields, is required to make more accurate prediction of their geoeffectiveness [e.g., Cane *et al.*, 2000].

In Figure 2, the temporary decrease in the rate of CME-related storms near solar maximum in 1980 and (less conspicuously) in 1990, deserves comment. In Richardson *et al.* [2000], we attributed the related depression in the averaged aa index in 1980 to the “Gnevyshev Gap”, a temporary decrease in the frequency of energetic solar events associated with the solar magnetic field reversal [e.g., Gnevyshev, 1967; Feminella *et al.*, 1997]. We also noted that this gap in geomagnetic activity is not caused by a changeover from CME-dominated to stream-dominated activity, as is also evident from Figure 2. Rather, there is a separate, later peak due to stream-related storms, which become prominent from

around two years after the gap occurs. Although previous studies have noted a “double peak” in storm activity near solar maximum [e.g., Gonzalez *et al.*, 1990], Figure 2 illustrates that this originates from the superposition of a double peak in the rate of CME-associated storms and a separate peak on the declining phase of the solar cycle caused by corotating streams, which may merge with the second CME-associated peak.

Acknowledgments. H.V.C. was supported at GSFC by a contract with USRA. I.G.R. was supported by NASA grant NCC 5-180. We acknowledge the use of OMNI and ACE near-Earth solar wind data supplied by the National Space Science Data Center and ACE Science Center respectively. The Kp data were obtained from the NOAA National Geophysical Data Center.

References

- Belcher J. N., and L. Davis Jr., Large-amplitude Alfvén waves in the interplanetary medium, 2, *J. Geophys. Res.*, **76**, 3534, 1971.
- Cane, H. V., I. G. Richardson, and T. T. von Rosenvinge, Cosmic ray decreases: 1964-1994, *J. Geophys. Res.*, **101**, 21,561, 1996.
- Cane, H. V., I. G. Richardson and O. C. St. Cyr, Coronal mass ejections, interplanetary ejecta and geomagnetic storms, *Geophys. Res. Lett.*, **27**, 3591, 2000.
- Cliver, E.W., Solar activity and geomagnetic storms: From M regions and flares to coronal holes and CMEs, *Eos Trans. AGU*, **76**(8), 75, 1995.
- Feminella, F., and M. Storini, Large scale dynamical phenomena during solar activity cycles, *Astron. Astrophys.*, **322**, 311, 1997.
- Gnevyshev, M.N., On the 11-years cycle of solar activity, *Sol. Phys.*, **1**, 107, 1967.
- Gonzalez, W. D., A. L. C. Gonzalez, and B. T. Tsurutani, Dual-peak solar cycle distribution of intense geomagnetic storms, *Planet. Space Sci.*, **38**, 181, 1990.
- Gosling, J. T., Coronal mass ejections and magnetic flux ropes in interplanetary space, in *Physics of Magnetic Flux Ropes*, *Geophys. Monogr. Ser.*, vol. 58, edited by C. T. Russell, E. R. Priest, and L. C. Lee, p. 343, AGU, Washington, D. C., 1990.
- Gosling, J.T., D.J. McComas, J.L. Phillips, and S.J. Bame, Geomagnetic activity associated with Earth passage of interplanetary shock disturbances and coronal mass ejections, *J. Geophys. Res.*, **96**, 7831, 1991.
- Richardson, I. G., and H. V. Cane, Regions of abnormally low proton temperature in the solar wind (1965-1991) and their association with ejecta, *J. Geophys. Res.*, **100**, 23,397, 1995.
- Richardson, I. G., H. V. Cane, and G. Wibberenz, Corotating cosmic ray depressions near the ecliptic during five solar minima: Evidence for a 22-year dependence, *J. Geophys. Res.*, **104**, 12,549, 1999.
- Richardson, I. G., E. W. Cliver, and H. V. Cane, Sources of geomagnetic activity over the solar cycle: Relative importance of CMEs, high-speed streams, and slow solar wind, *J. Geophys. Res.*, **105**, 18,203, 2000.
- St. Cyr, O. C. *et al.*, Properties of coronal mass ejections: SOHO LASCO observations from January 1996 to June 1998, *J. Geophys. Res.*, **105**, 18,169, 2000.
- Tsurutani, B. T., and W. D. Gonzalez, The interplanetary causes of magnetic storms: A review, in *Magnetic Storms*, *Geophys. Monogr. Ser.*, vol. 98, edited by B. T. Tsurutani *et al.*, p. 77, AGU, Washington, D. C., 1997.

H. V. Cane and I. G. Richardson, Code 661, Laboratory for High Energy Astrophysics, NASA Goddard Space Flight Center, Greenbelt, MD 20771. (hilary.cane@utas.edu.au; richardson@lheavx.gsfc.nasa.gov)

E. W. Cliver, Space Vehicles Directorate (VSBXS), Air Force Research Laboratory, Hanscom AFB, MA 01731-3010. (cliver@plh.af.mil)

(Received February 20, 2001, accepted April 13, 2001.)